

# Decay of Wake Vortices of Large Aircraft

Turgut Sarpkaya\*

U.S. Naval Postgraduate School, Monterey, California 93943

A brief summary of previous works is followed by an in-depth analysis of velocities, circulations, and decay histories of a number of trailing vortices generated by large aircraft during field tests in Memphis, Tennessee. The results suggest that the decay of trailing vortices is governed by the mutual straining of vortices; intermittent exchange of mass, momentum, and vorticity across the core boundary; rotational damping and restructuring of turbulence in the core; stretching of large turbulent structures, turbulent diffusion, and the interaction of oppositely signed vorticity in the overlapping regions of the vortex pair; and the draining of vorticity from the Kelvin oval.

## Nomenclature

$b_0$	= initial separation of vortices
$c$	= chord length
$k$	= turbulent kinetic energy
$N$	= number of scanned sections
$Rcn$	= core radius at $n$ th scanned section
$Rcv$	= average of $Rcn$ over $N$ scanned sections
$Rc1$	= core radius at the first scanned section
$Rec$	= Reynolds number based on circulation, $\Gamma/v$
$Rev$	= Reynolds number based on velocity, $V_m Rcv/v$
$Ro$	= Rossby number, $(U_\infty - U_{cl})/V_m$
$r$	= radial distance
$r^*$	= $r/Rcv$
$T^*$	= $V_0 t/b_0$
$t$	= time (measured from the wing)
$t^*$	= $V_m t/Rcv = \omega t$
$U$	= axial velocity
$U_{cl}$	= axial centerline velocity
$U_\infty$	= axial ambient velocity
$V_m$	= maximum $v$ at $r^* = 1$
$V_0$	= $\Gamma/(2\pi b_0)$
$v$	= tangential velocity
$v^*$	= $v/V_m$
$x$	= axial distance
$z$	= vortex elevation
$\Gamma$	= circulation of vortex, $2\pi r v$
$\Gamma_{av}$	= average of $\Gamma$ between $Rc1$ and $r^*$
$\Gamma_{av}^*$	= $\Gamma_{av}/(2\pi Rcv V_m)$
$\varepsilon$	= dissipation
$\varepsilon^*$	= $(\varepsilon b_0)^{1/3}/V_0$
$\Lambda$	= dissipation length
$\nu$	= kinematic viscosity
$\Omega$	= vorticity, $\Gamma/\pi r^2$
$\Omega^*$	= normalized vorticity, $\Omega Rcv/V_m$
$\omega$	= angular velocity of the core, $t^*/t$

## Introduction and Brief Review

THE current impetus for research on single and mutually straining vortices comes, in part, from the need to enhance the capacity of large airports by reducing wake-hazard-imposed aircraft separations for various flight modes and meteorological conditions. A review of the extensive literature<sup>1-3</sup> indicates that there are major obstacles to an understanding of the physics of trailing vortices for the prediction of their transport and decay, for the promotion of their

receptivity to instability, and for the rapid reduction and spreading of their vorticity into random turbulence. The interaction of vortices with what surrounds them and the relation between the full-scale flight tests and the physical/numerical laminar-flow experiments remain elusive. A brief summary of the principal obstacles is given next.

1) Pre-roll-up history: As noted by MacCready,<sup>4</sup> "anything altering the thickness, turbulence, and longitudinal velocities in the vortex sheet out of which the core is formed can be expected to alter its characteristics." More recently, this realization led to the exploration of the possibility that one might be able to precipitate the breakup of the rolled-up vortices by relatively small and judiciously selected local unsteady forcing imposed on the shear layers before their roll-up.<sup>5</sup> It is hoped that this process will require relatively small energies to trigger wake instabilities that harness the wake energy for its own destruction. Some of the possibilities that could help to intensify turbulent diffusion and reinforce the decay mechanisms are a) to sandwich more turbulence into the rotational/irrotational layers during their roll-up to enhance Helmholtz and Rayleigh instabilities in the discontinuous (sawtooth-like) velocity profiles, to increase the core radius and the overlapping of the oppositely signed vorticity, and to precipitate Crow instability and linking; b) to use structural modifications along the trailing edges of the wings and flaps, e.g., in the form of sinusoidal profiles, to enhance the three-dimensionality of the flow and turbulence in the shear layers after their roll-up, to unload the outboard segments of the wings to reduce the wing tip vorticity, i.e., to reduce the fraction of circulation that is within the core and to increase the axial velocity; and c) to utilize the thrust system to diffuse the shear layers. So far, the efforts to excite the shear layers or to modify the aircraft design did not lead to benign vortex wakes either in cruising or in landing/takeoff situations.

2) Post-roll-up circumstances: It has been clear for quite some time that stratification, shear, turbulence, and instabilities from all sources with their direct or indirect consequences are the fundamental demise mechanisms that destroy the coherence of a vortex wake.<sup>6</sup> The preexisting turbulence has a strong influence on the stability and on the gradual and/or catastrophic demise of vortices.<sup>7,8</sup> However, preexisting turbulence is difficult to quantify, particularly before each flight. The physics of the decay mechanism resulting from the interaction of the ambient turbulence with the vortex is not understood; it is only inferred from the migration and lifespan of vortices in small-scale experiments conducted in grid-generated turbulence.<sup>8,9</sup> In spite of its major importance, there has never been an experiment, at any scale, where the distributions of mean flow-field and the complete Reynolds stress tensor were measured at numerous sections downstream from the wing tip, immersed in a known, e.g., grid-generated, turbulence field.

The ambient turbulence may be characterized by its kinetic energy  $k$  per unit mass and its dissipation rate  $\varepsilon$  ( $k$  or  $\varepsilon$  may be replaced by the dissipation length  $\Lambda$ , defined by  $\Lambda = k^{3/2}/\varepsilon$ , where  $\Lambda/b_0$  is a measure of the dominant eddy size). In addition, dissipation needs a structural intermittency correction because the preexisting

Received Dec. 8, 1997; presented as Paper 98-0592 at the AIAA 36th Aerospace Sciences Meeting and Exhibit, Reno, NV, Jan. 12-15, 1998; revision received April 14, 1998; accepted for publication April 22, 1998. This paper is declared a work of the U.S. Government and is not subject to copyright protection in the United States.

\*Distinguished Professor of Mechanical Engineering, Department of Mechanical Engineering, 700 Dyer Road. E-mail: Sarp@nps.navy.mil. Associate Fellow AIAA.

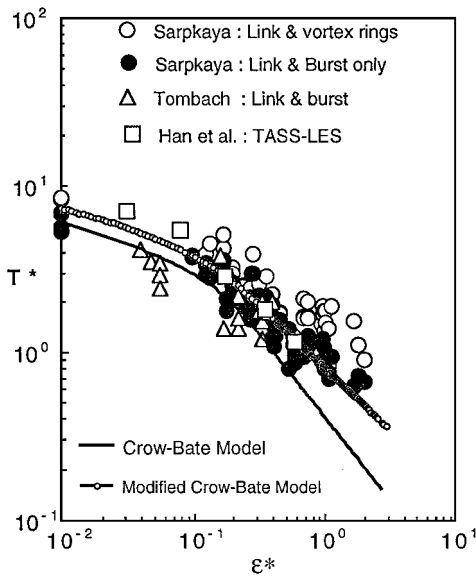


**Fig. 1**  $T^*$  vs  $\varepsilon^*$ : models and physical and numerical experiments.

atmospheric turbulence is not a random sea of uncorrelated structures but rather is one that exhibits highly localized vorticity events.

The turbulence parameter  $\varepsilon^*$ , defined by Crow and Bate<sup>10</sup> with  $V_0 = \Gamma/2\pi b_0$ , was subsequently used by Tombach<sup>7</sup> and Sarpkaya and Daly<sup>8</sup> in their work on trailing vortices. Figure 1 shows  $T^*$  vs  $\varepsilon^*$  for two sets of experimental data,<sup>7,8</sup> two analytical predictions (the Crow and Bate<sup>10</sup> model and the one modified herein), both based on the original analysis of Crow,<sup>11</sup> and the results of the large eddy simulation of the lifetimes-to-linking by Han et al.<sup>12</sup> (all for a nonstratified medium).

In weak turbulence (i.e., for  $\varepsilon^*$  less than about 0.02 or for  $\varepsilon$  less than about  $0.03 \text{ cm}^2/\text{s}^3$  for a DC-10-30 with  $\Gamma = 544 \text{ m}^2/\text{s}$  and  $b_0 = 37 \text{ m}$ ), multiple linking (with an average wavelength of about  $7.8b_0$ ) and the subsequent instability events destroy the coherence of vortices. In medium turbulence (i.e., for  $\varepsilon^*$  greater than about 0.02 and less than about 0.2 or for  $\varepsilon$  less than about  $30 \text{ cm}^2/\text{s}^3$  for a DC-10-30), the dominant form of instability is the Crow instability (with decreasing wavelengths and integral length scales) and occasional vortex bursting. The physics of the latter is not understood, but it is known that bursts do not lead to reconnection. Finally, for stronger turbulence (i.e., for  $\varepsilon^*$  larger than about 0.3 or 0.4, up to as large as 2), vortex bursting, all other forms of instability, strong mixing in the overlapping region of the vortices, roll-up of vortices about each other, and lateral displacements spread the vorticity irreversibly over a large area.<sup>6,8</sup>

Figure 1 shows that the Crow and Bate<sup>10</sup> model serves as a lower bound to the link/burst data. It becomes inadequate for  $\varepsilon^* > 0.2$  where the predicted decay is quite steep. The reasons lie in the highly restrictive nature of some of the assumptions made in their pioneering analysis. The most important ones are that eddies as large as  $8.6b_0$  lie in the inertial subrange, the atmospheric turbulence is regarded as independent of the vortices, and the lifespan is determined by extrapolating the linear theory to times when the displacement perturbations are comparable to  $b_0$ . As noted earlier, both the wavelength and the integral length scale decrease with increasing  $\varepsilon^*$ , at least in small-scale experiments. Crow and Bate<sup>10</sup> drew attention to the fact that “there seems to be no straightforward way to handle such departures, and the assumption that they are unimportant will have to be tested by comparing the calculated lifespans to experiment.” It is in accordance with their suggestion that the Crow and Bate<sup>10</sup> model has been rederived to allow for the variation of the wavelength and the integral length scale. The resulting vortex lifespans in strong and weak turbulence are given by

$$\varepsilon^* T^{*4/3} = \frac{3}{4} \quad \text{for} \quad T^* < 2.5 \quad (1)$$

and

$$\varepsilon^* = T^{*1/4} \exp(-0.70T^*) \quad \text{for} \quad T^* > 2.5 \quad (2)$$

and are depicted in Fig. 1 as the modified Crow–Bate model.

Equation (2) is very similar to the original equation (15) of Crow and Bate.<sup>10</sup> However, Eq. (1) differs somewhat from the original one [Eq. (6)] to allow for the interaction of strong turbulence with the vortices. Clearly, the data are better represented by Eqs. (1) and (2). Furthermore, the rederived model appears to be in better agreement with the predictions of Han et al.<sup>12</sup>

The linking of the vortices is followed by the formation of crude vortex rings and azimuthal instabilities. This process appears to precipitate the destruction of wake vortices even though it does not necessarily reduce the wake hazard. There are no reliable data at aircraft scales to assess the significance of the vortex rings and the structure of the resulting vorticity distribution. In Fig. 1, only the data identified as link and vortex rings (open circles) include the time to the disappearance of vortices in laboratory scales.

In Memphis tests, the turbulence or turbulent kinetic energy (TKE) data (1 min averaged) were taken at a height of 40 m (Ref. 13). In JFK tests, similar data were taken at 5 m. Even though it is theoretically possible to obtain an estimate of the spectral energy density (using the 5- and 40-m data) and thereby to calculate the dissipation rate directly, one obtains only an average over a height of 40 m. What is needed is the dissipation from the near-ground level to several hundreds of meters up to provide reliable input to the numerical simulations. Note that  $\varepsilon^*$  is the ratio of the rms velocity difference between two fluid particles separated a distance  $b_0$  in the inertial subrange to the mutual induction velocity of the vortices. This information, however desirable, cannot be readily obtained from the available field data.<sup>13,14</sup> It might be necessary to resort to  $\varepsilon$  and  $\varepsilon^*$  values noted earlier, after subjectively classifying the ambient turbulence as mild, medium, and strong on the basis of  $k$  values and other meteorological data. A comparison of the computed and observed vortex characteristics might then help to calibrate the dissipation values to be used. It appears that the laminar/turbulent question regarding the structure of flow surrounding an aircraft vortex is much too complex and may need to be described in terms of  $x/c$ ,  $(\varepsilon b_0)^{1/3}/V_0$ ,  $V_0 b_0/\nu$ , and  $k^{1/2}/V_0$ . The existence of the axial velocity (jet like or wake like) is thought to be indispensable but so far remains unquantified.<sup>15–20</sup> It is often expressed in terms of the Rossby number, suitably defined in terms of the axial and maximum tangential velocities, e.g., axial velocity defect/maximum tangential velocity.<sup>19</sup>

3) Experimental limitations: Even the highest Reynolds numbers ( $Rec = \Gamma/\nu$ ) reached in wind tunnels or towing basins (typically,  $Rec = 4 \times 10^4$ ) are several orders of magnitude lower than what is possible for an aircraft, e.g.,  $Rec = 3.6 \times 10^7$  for a DC-10-30. It is rather unfortunate that all of the governing decay parameters cannot be realized in small-scale laboratory experiments and direct numerical simulations. However, small-scale experiments and numerical simulations have drawn attention to the physics of some of the most fundamental mechanisms.<sup>6–9,12,20–24</sup>

In recent years, continuous-wave coherent laser Doppler radar (Lidar) measurements, coupled with the simultaneous recording of the environmental conditions, provided the most reliable database so far from which one could extract accurate enough information on velocity, circulation distribution, displacement, decay, angular momentum, kinetic energy, and lifetimes of the vortices and on the effects of wind, shear, ground, stratification, humidity, and precipitation.<sup>13,14</sup> It is hoped that these data will lead to a better understanding of the decay mechanisms of field vortices and to a careful assessment, validation, and improvement of the numerical simulations, preferably the large-eddy simulation (LES). However, the field data are not free from a number of shortcomings. The most important ones are that the preexisting TKE levels for the Memphis data are not available at elevations higher than 40 m, dissipation is not given and is difficult to estimate, there is no information on axial velocities, and the tangential velocity needs to be corrected carefully. However, there are, at present, no better alternatives to the field data in search of a solution of the wake–vortex hazard problem.

Detailed uncertainty analysis of the Memphis data is given by Zak and Rogers,<sup>13</sup> Campbell et al.,<sup>14</sup> and Heinrichs and Dasey<sup>25</sup> and will not be repeated here because of space limitations. Suffice it to note that an appreciation of these facts, together with the fact that the current field data represent the state of the art, is of special importance in assessing the results presented herein. They deal only with

the data that gave rise to them and not with the great controversies surrounding the core size and the circulation decay.

Evaluation of the Data

The data set discussed herein (Table 1) comes from the Memphis Field Program<sup>14</sup> conducted during December 1994 and August 1995 at Memphis, Tennessee, as part of the larger effort by the NASA Langley Research Center to develop an Aircraft Vortex Spacing System<sup>26-30</sup> as an element of the Terminal Area Productivity program. Its purpose is to minimize the scientific uncertainty about wake vortex behavior under different atmospheric conditions to develop a safe and adaptive vortex spacing system.

The selection of the flights shown in Table 1 was based on a number of factors: landings of the same type of aircraft, whenever possible, in both the low and relatively high *k* conditions (M-1252 and M-1581, M-1170 and M-1583), the large number of measurement sections in both the port and starboard vortices, the steadiness of the relative positions of the vortices during the time of Lidar measurements, and consistency of the velocities, as seen in the preliminary plots.

First, all velocities were corrected for the effect of the neighboring vortex (including the changes in vortex spacing) using straightforward hydrodynamic considerations (line-vortex assumption and Biot-Savart law) devised by Heinrichs and Dasey.<sup>25</sup> The calculations of relative circulation in terms of the vortex pair separation, for various average circulations (radius averaging<sup>25</sup>), have shown that the farther from the core that the averaging extends and the smaller the wingspan of the test aircraft, the larger the effect of the vortex-vortex proximity; e.g., for a DC-10, the relative increase in estimated circulation is about 10%, and for a B-757, it increases to about 15%. Detailed numerical analysis of the effect of mutual straining of the vortices on the velocity and circulation distributions has shown that the effect of the environmental conditions on the decay of circulation is an order of magnitude larger than that of the mutual straining of the vortices. In fact, an iterated analysis of several flights listed in Table 1 has shown conclusively that the integration of the 15-m averaged circulation consistently reproduces the independently measured vortex elevation *z*, given by

$$z = \frac{1}{2\pi b_0} \int \Gamma_{av} \, dt \tag{3}$$

The data were also corrected for the wind, shear, vortex descent, core radius, maximum velocity at the edge of the core, and ground proximity (if warranted). Some of these corrections are rather straightforward. For example, the uniform-wind correction is made by adding to or subtracting from the proper half of the vortex the component of the wind velocity along the line of sight. The correction for shear was made with as much care as possible by properly adding the shear profile to the velocity profile of the vortex at discrete radial distances. As expected, the effect of the shear was to increase the circulation of one vortex and to decrease that of the other. If the relative positions of the port and starboard vortices did not reflect the expected changes (either because the correction was too small or because the shear was not uniformly valid over the lateral space), the correction was ignored. As correctly emphasized by one of the referees, the correction procedure is predicated on the assumption of the horizontal coherence of the wind field. This, of course, is not always the case, and the correction for shear has to be made with great care.

Table 1 Some characteristics of the flights analyzed				
Flight number	Aircraft	<i>k</i> , m <sup>2</sup> /s <sup>2</sup>	Γ <sub>0</sub> , m <sup>2</sup> /s	Wing span, m
M-1257	DC-10	0.01	406	50.4
M-1267	DC-10-10	0.07	483	47.3
M-1273	DC-10-30	0.01	544	47.3
M-1279	DC-10-30	0.05	531	50.4
M-1252	B-757	0.023	435	37.9
M-1581	B-757	1.21	370	37.9
M-1170	EA-320	0.02	325	33.9
M-1583	EA-320	2.93	291	33.9

For all of the flights evaluated, the effect of filtering the velocity data using the five-point filtering technique of Longuet-Higgins and Cokelet<sup>1</sup> [i.e.,  $v_i = (-v_{i-2} + 4v_{i-1} + 10v_i + 4v_{i+1} - v_{i+2})/16$ ] was assessed, and it was found that, although the velocity and circulation profiles become somewhat smoother, the decay characteristics of the circulation at a given radius with time or at a given time with *r* (radial distance) do not measurably change.

The final correction to the velocity profiles stems from the fact that the coordinates of the Lidar data do not necessarily coincide with the correct vortex center. The proper coordination of the two halves of the velocity profiles requires the calculation of the core radii. To this end, the absolute values of the left and right sides of the velocities (already corrected for wind, shear, etc.) are plotted as a function of 1/*r* (Fig. 2) to determine the apparent core radius. Then the average of the left and right core radii is determined, and the total velocity profile is shifted along the *r* axis as required (often by small amounts) to place the origin of the coordinate axis at the correct center of the vortex at the time of its scanning (Fig. 3). Note that the core radius of a vortex does not appreciably change during the time interval of the Lidar measurements (often under 2 min), and the exact size

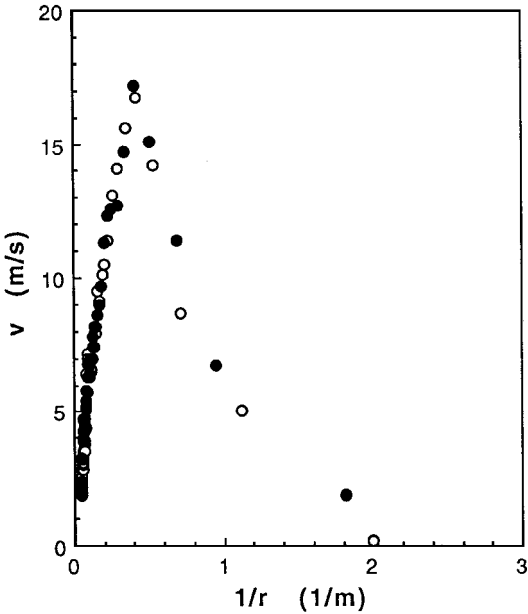


Fig. 2 Plot of typical tangential velocity vs *r*<sup>-1</sup>.

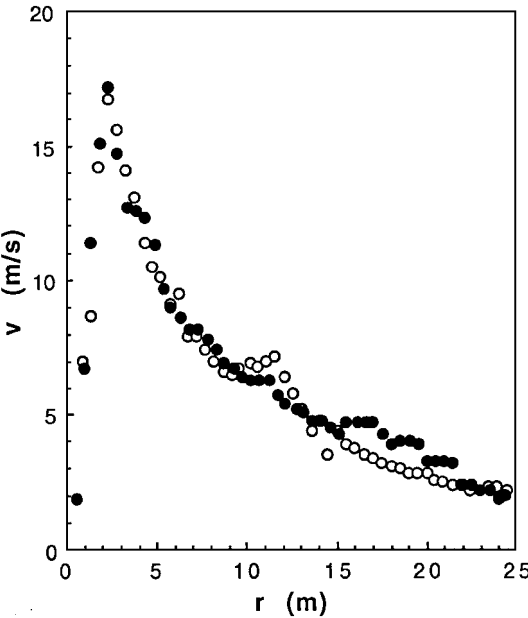


Fig. 3 Two halves of the corrected tangential velocity.

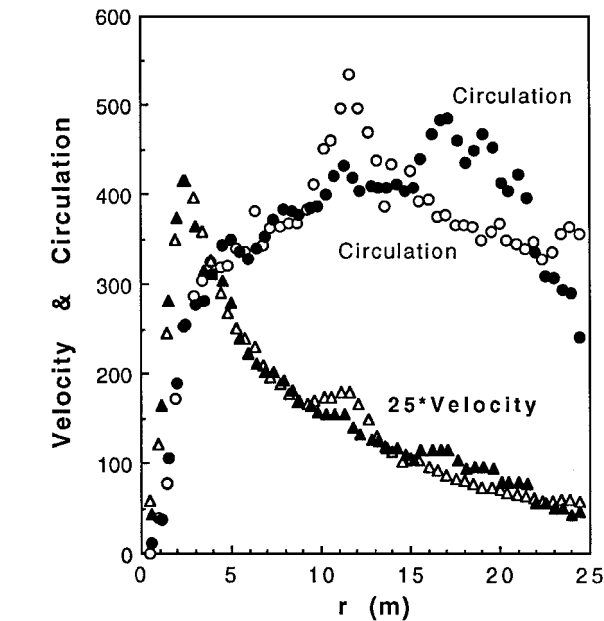


Fig. 4 Typical velocity and circulation distributions.

of the core is not of particular importance as far as the circulation decay is concerned. Once the velocity profiles are corrected, the circulation, vorticity, and all other variables of interest derivable from them are plotted in dimensional as well as dimensionless forms. For example, Fig. 4 shows that the circulation can exhibit relatively large fluctuations in spite of the apparent smoothness of the velocity profiles (larger velocities at smaller radii and smaller velocities at larger radii). This fact must be kept in mind in deducing information from the circulation data.

Results and Discussion

A study of this type produces numerous plots even for a single flight. It is for this reason that only the data most relevant to the conclusions are presented here. Furthermore, they are plotted in either normalized or dimensional forms and as either actual or averaged values (not necessarily both) to convey some practical information about the magnitudes of the actual circulations as well as their averaged values. Note that the data presented herein are for vortices generated out of the ground effect. In the following, first the data for the individual flights are discussed, and then a more detailed comparison of some of the flights is made.

Figures 5–10 show the results of four DC-10 flights (see Table 1). These flights were executed at relatively low TKE levels, and there were no DC flights (in the Memphis data) in higher TKE conditions. Figure 5 shows the averaged circulation<sup>25,32</sup>  $\Gamma_{av}$  (from  $Rc1$  to  $r$ ) for M-1257 as a function of time at four radial distances from the vortex center. Even though  $\Gamma_{av}$  does not, at a given time, significantly vary with  $r$  at the four radii shown, it decays with time at all radii. Figure 6 shows the normalized average circulation  $\Gamma_{av}^*$  as a function of the normalized time  $t^* (= \omega t)$  for M-1267 at four  $r^*$ . The term  $\Gamma_{av}^*$  exhibits three distinct regions. For  $t^*$  less than about 300, there is a rapid decay in  $\Gamma_{av}^*$  with time at all radii. This is partly due to the rapid turbulent diffusion of vorticity out of the core (to be discussed more later) and partly due to the normalization of  $\Gamma_{av}^*$  with  $Rcv$ . (Note that the minimum  $r^*$  in Fig. 6 is 1.25.) In the approximate interval of  $300 < t^* < 1100$ , the decay is relatively small, and for  $t^*$  larger than about 1100, there is again a rapid decay. Figure 7 is a typical example of the decay of maximum circulation with time for M-1279. This is one of the flights where the decay of circulation at a given time with  $r$  is as large as that at a given radius with time. The circulation increases up to  $r = 12$  m and then decreases for all  $r$  larger than about 15 m.

The next three figures concern M-1273 (a DC-10-30). Figures 8 and 9 show the maximum and the normalized average circulation, respectively, at four representative radii. The magnitude of the initial circulation in Fig. 8 is sufficient to draw serious attention to the

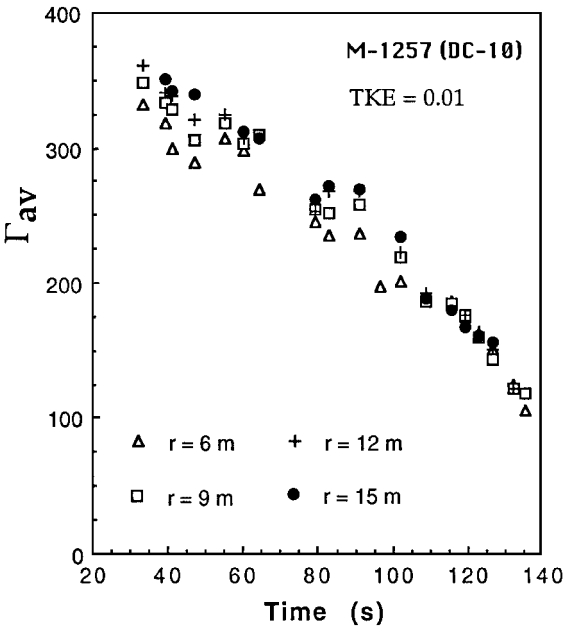


Fig. 5 Averaged circulation vs time for M-1257.

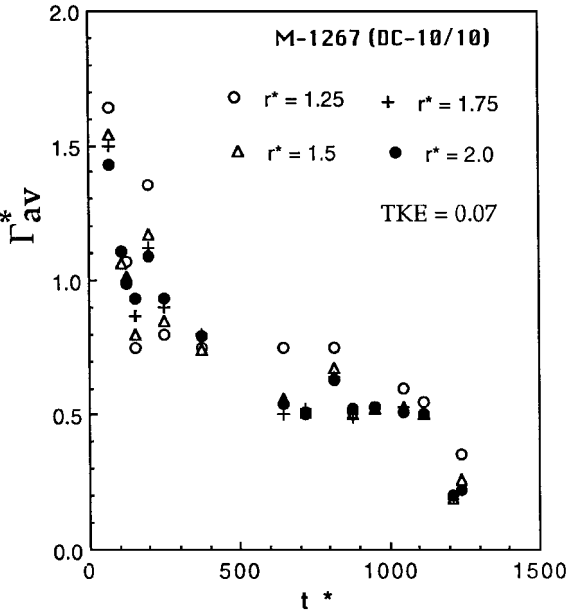


Fig. 6 Normalized average circulation vs  $t^*$  for M-1267.

magnitude of the wake-hazard problem. Figure 9 is quite similar to previous ones in all of its characteristics. The strength of the vortices reduces to about one-third of their initial values by  $t^* = 1000$  and then continues to decay for a while longer. It is also noted that all of the foregoing flights exhibit, to varying degrees, three distinct time intervals, as in Fig. 6, where the decay experiences a rapid-slow-rapid rate with time.

Figure 10 shows the decay of the normalized vorticity  $\Omega^* [= (\Gamma/\pi r^2)(Rcv/V_m)]$  as a function of  $r^*$  at four  $t^*$  values. The first point on each curve represents the edge of the vortex core (taken as the point at which the velocity is maximum). At  $t^* = 80$  (the starting time of the Lidar measurements in this flight), the initial core radius is  $Rc1 = 2.5$  m. It increases only to 3.1 m at  $t^* = 1336$ , the time of the last Lidar measurement. Clearly, the vorticity decays with increasing time and radial distance, a fact that is consistently observed in all flights reported herein. In dimensional terms, the vorticity in the core of the vortex shown in Fig. 10 reduces to one-quarter of its initial value in about 155 s. A laminar vortex of identical initial strength and core radius would have required at least 10 h to undergo a similar decay through molecular diffusion and core expansion. All

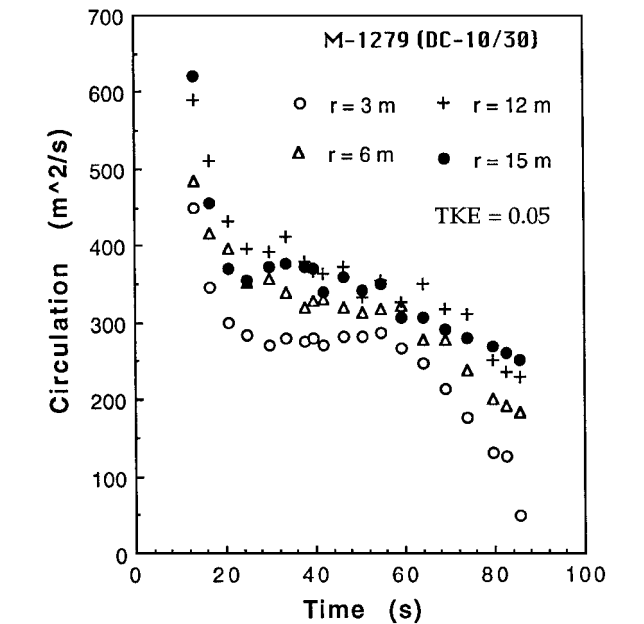


Fig. 7 Circulation vs time for M-1279.

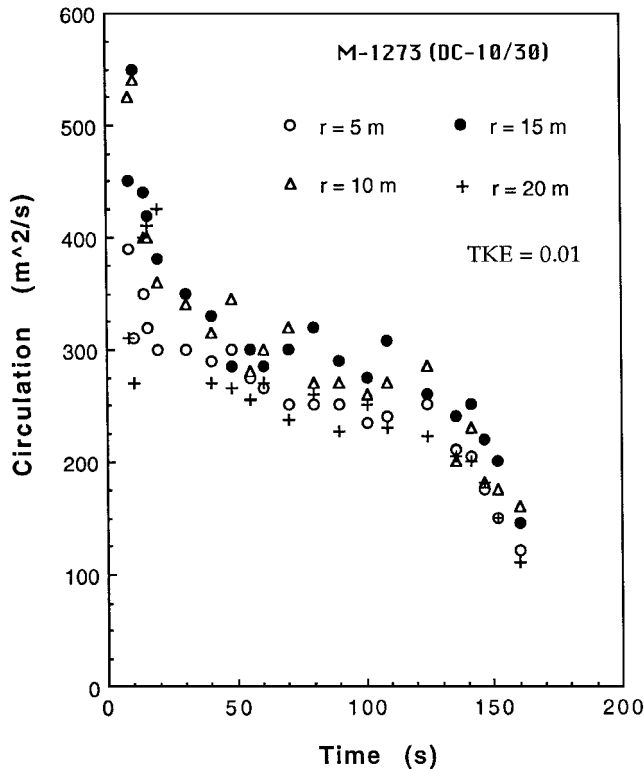


Fig. 8 Circulation vs time for M-1273.

of the other flights discussed herein led to molecular diffusion times an order of magnitude larger than those observed and recorded in the field experiments. In fact, if one were to use a crude turbulent eddy viscosity model, in predicting diffusion through the use of the classical diffusion equation,  $\nu_t$  would have to be 200–500 times larger than the kinematic viscosity to bring the said decay into satisfactory agreement with the field measurements. According to the data from various investigators,<sup>33,34</sup> estimates for  $\nu_t/\nu$  fall between 30 and 2000, depending on  $Rec$ . Clearly, laminar diffusion mechanisms are not relevant to the prototype aircraft vortices, and more powerful diffusive as well as nondiffusive mechanisms must be at work even when the preexisting turbulence and stratification effects are negligible, as in the case of M-1273 (see Table 1).

Figures 11 and 12 show the  $\Gamma$  and  $\Gamma_{av}^*$  in terms of  $t$  and  $t^*$ , respectively, for two B-757 flights. Figures 13 and 14 are for two

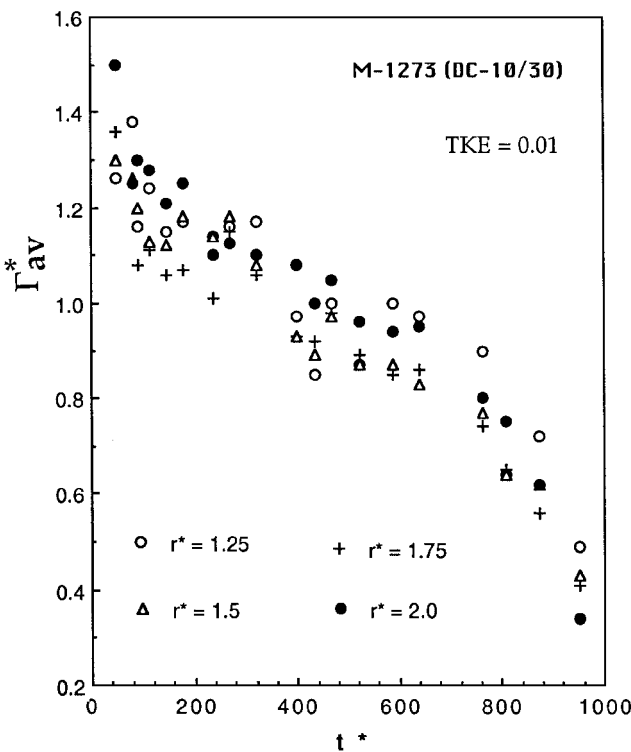


Fig. 9 Normalized average circulation vs  $t^*$  for M-1273.

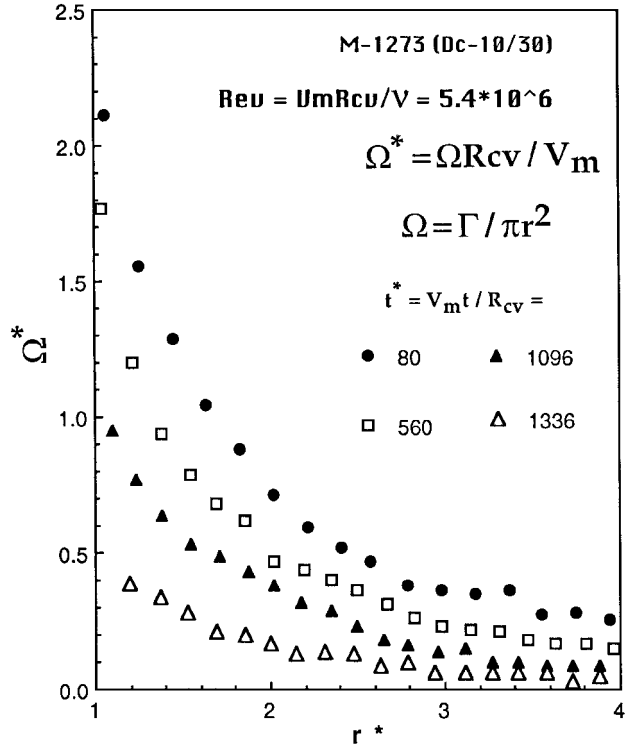


Fig. 10 Normalized vorticity vs  $r^*$  for M-1273.

EA-320 flights and show  $\Gamma$  as a function of time. The differences between the decay rates and durations of the two flights are due to the fact that  $k = 0.02 \text{ m}^2/\text{s}^2$  for M-1170 (Fig. 13) and  $k = 2.93 \text{ m}^2/\text{s}^2$  for M-1583 (Fig. 14).

Figures 15–17 show specific comparisons of some of the flights discussed earlier. The decay of circulation of the two DC-10-30 flights at  $r^* = 2$  is shown in Fig. 15. The TKE levels for M-1273 and M-1279 are 0.01 and  $0.05 \text{ m}^2/\text{s}^2$ , respectively. In the absence of any other strong meteorological factors, the faster decay and shorter life of the circulation of M-1279 may be attributed to the fact that it

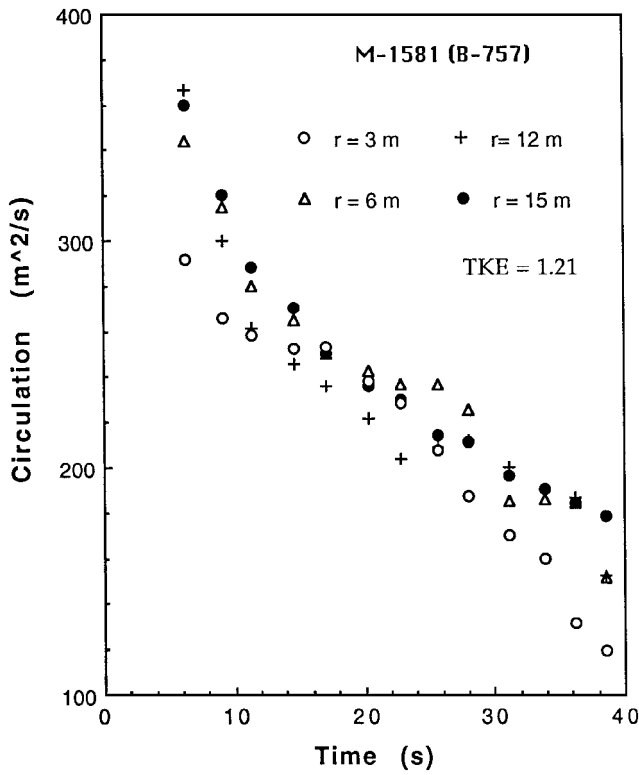


Fig. 11 Circulation vs time for M-1581.

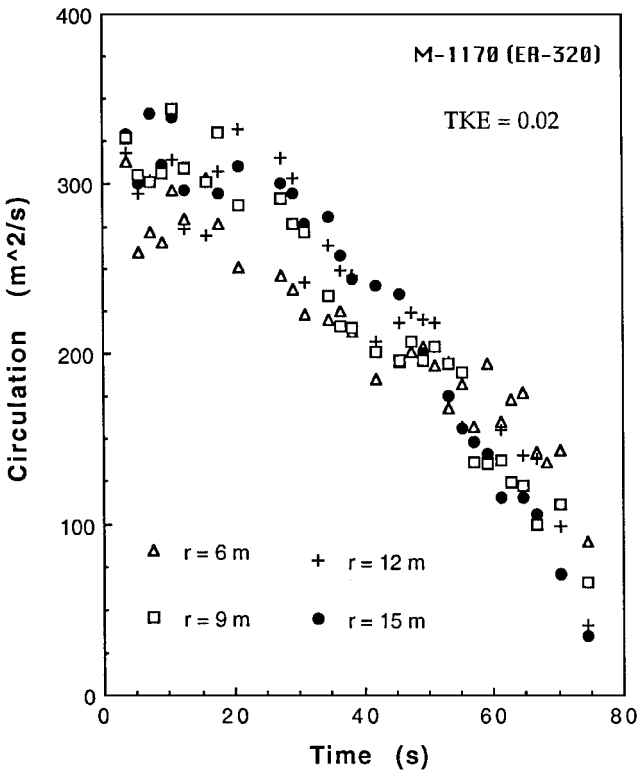


Fig. 13 Circulation vs time for M-1170.

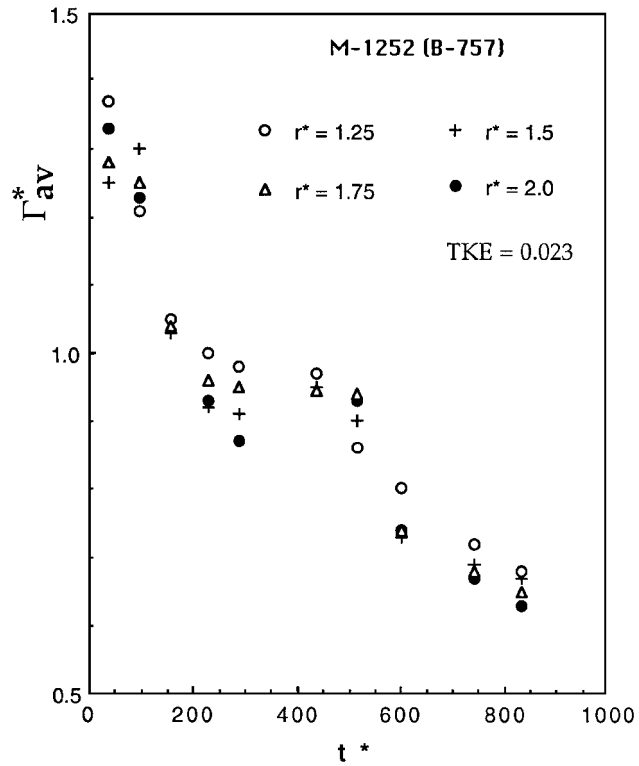


Fig. 12 Normalized average circulation vs  $t^*$  for M-1252.

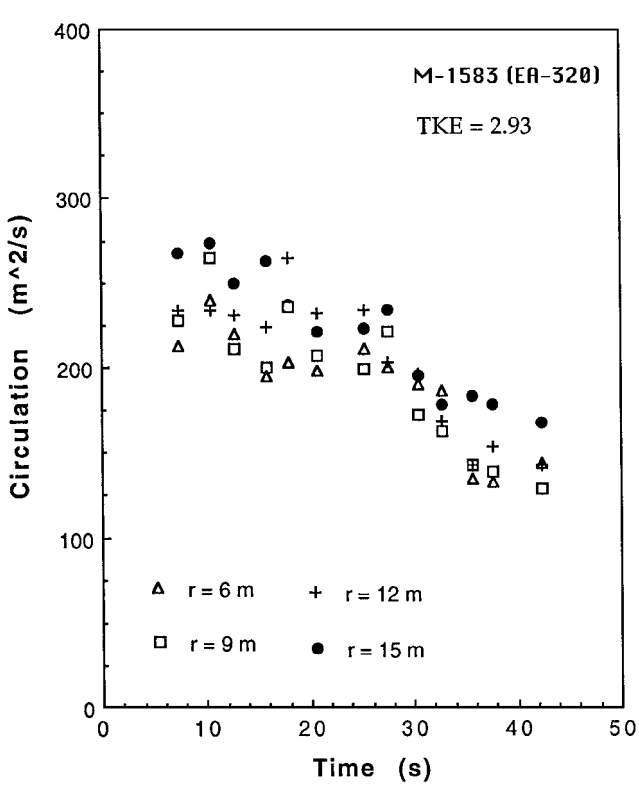


Fig. 14 Circulation vs time for M-1583.

has experienced a five-times-larger TKE level. The comparison of the circulations of M-1252 ( $k = 0.023$ ) and M-1581 ( $k = 1.21 \text{ m}^2/\text{s}^2$ ) is shown in Fig. 16. The significant differences between their decay rates and lifetimes are evident not only at  $r = 7.5 \text{ m}$  (the radius depicted in Fig. 16) but also at all other radii, not shown here. Figure 17 shows a similar comparison between M-1170 ( $k = 0.02 \text{ m}^2/\text{s}^2$ ) and M-1583 ( $k = 2.93 \text{ m}^2/\text{s}^2$ ) at  $r = 7.5 \text{ m}$  for two EA-320 flights. The effect of the higher turbulence level is indeed in conformity with the expectations.

It is clear from the foregoing that the decay of trailing vortices is significantly different from that of laminar vortices. Neither the uncertainties in the atmospheric conditions nor the shortcomings of the Lidar measurements are large enough to alter the basic conclusion. A nonmolecular diffusion process has to be constructed to explain the observations and measurements, to construct model equations (similar to that pioneered by Greene<sup>35</sup>), and to provide guidance to numerical simulations.<sup>28,29</sup>

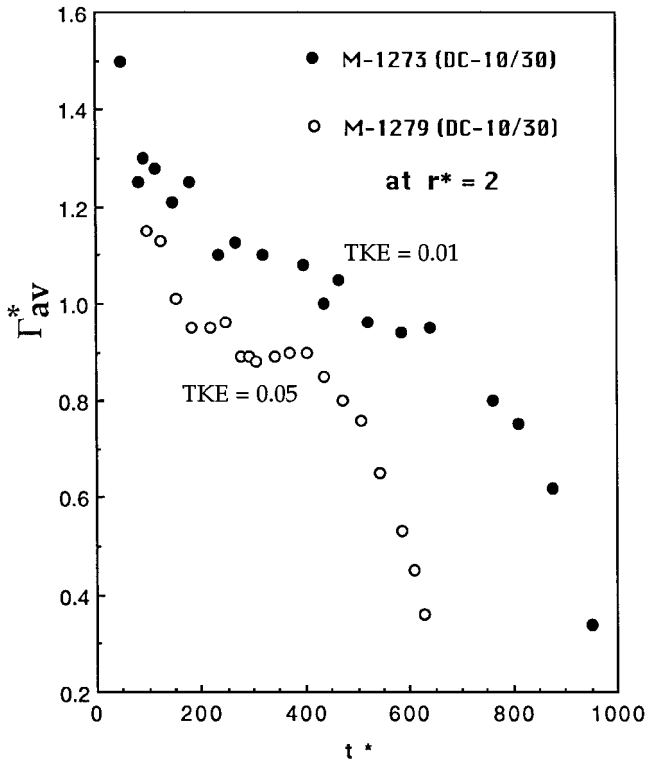


Fig. 15 Normalized average circulation vs  $t^*$  for M-1273 and M-1279.

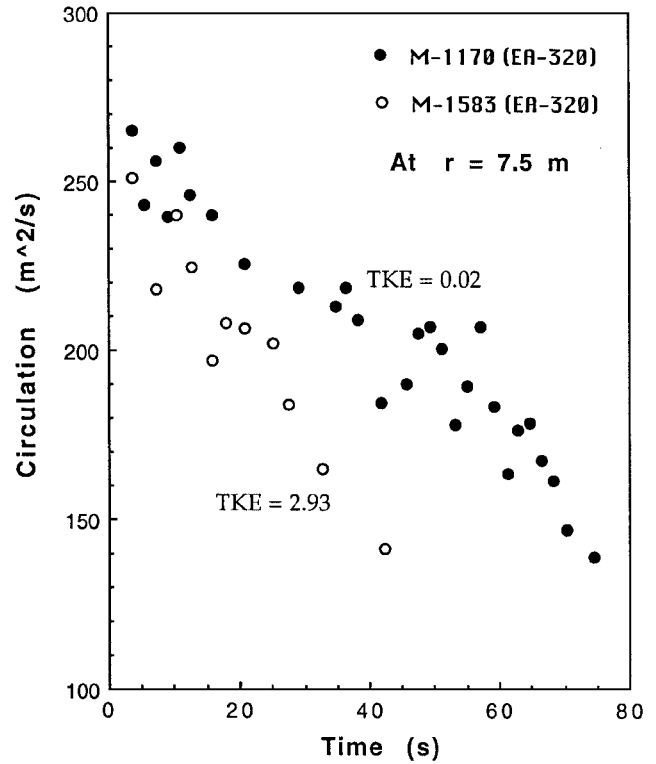


Fig. 17 Circulation vs time for M-1170 and M-1583.

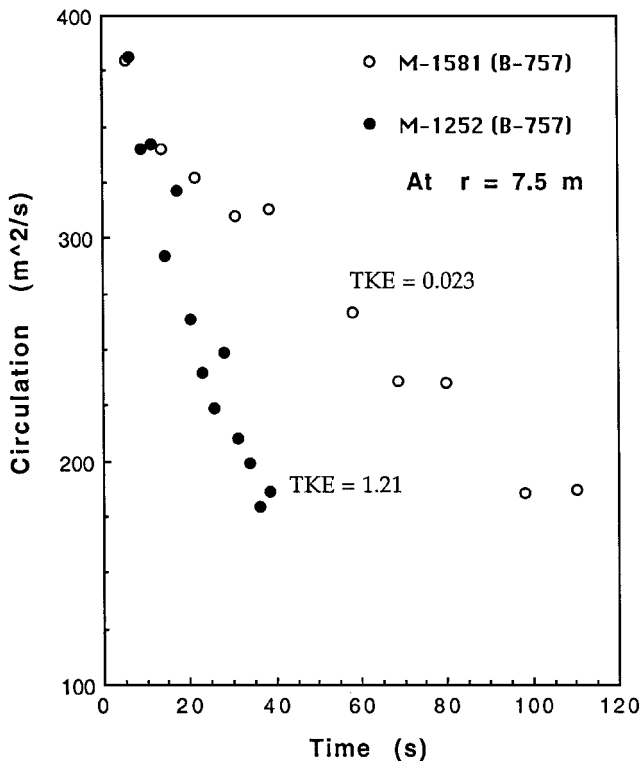


Fig. 16 Circulation vs time for M-1581 and M-1252.

Figures 6, 9, and 12 show that the circulation near the edge of the core does not remain constant. In fact, Fig. 10 shows that the vorticity at the edge of the core decays with time (at an increasing rate), whereas the core radius changes only from about 2.5–3.1 m. Had the circulation remained constant at the edge of the apparent core, the average vorticity would have decreased by only 35% relative to its initial value. In Fig. 10 the vorticity in the core decreases by about 80%. Similar calculations for all other flights led to the conclusion that the vorticity is not locked up in the core by the

lack of turbulence, notwithstanding the arguments of Hallock and Burnham<sup>32</sup> to the contrary.

This calls for a careful examination of the behavior of the core and its interaction with its surroundings. The first phase of the interaction concerns the early stages of the roll-up process where the core is still composed of rolled-up vortex sheets with strong (sawtooth-like) velocity discontinuities. These are susceptible to Helmholtz and Rayleigh instabilities and give rise to turbulence that, in turn, smooths the velocity discontinuities. It is emphasized that this turbulence is generated within the core, not imported from the environment. The later stages of the evolution of the core concern the simultaneous effects of the smoothing action of the rotation and the vorticity exchange between the inner and outer regions of the core.

The rotational damping of turbulence is not, of course, a new idea. For example, Traugott<sup>36</sup> has shown, by measurements of screen-produced turbulence between rotating concentric cylinders, that rotation produces more rapid growth of the boundary layer on the inner or convex surface while retarding growth of the boundary layer on the outer concave surface. The measurements of Briggs<sup>37</sup> with a rotating pipe flow suggested that increasing the angular velocity of the enclosing pipe delays the transition within the pipe from laminar to turbulent flow. The experiments by Hopfinger et al.<sup>38</sup> have shown that the normal cascade of coherent structures in a rotating flow is in favor of the appearance of coherent structures. Hopfinger et al. reported a dramatic transition in the turbulent flowfield when the local Rossby number was decreased below 0.2, with a collection of coherent vortices appearing with their axes approximately parallel to the rotation axis. Polifke and Shtilman,<sup>39</sup> among others, have shown that high levels of helicity tend to retard the cascading of turbulent energy to smaller scales and thus reduce dissipation. It is reasonable to conclude that the turbulence in the core of a trailing vortex is subjected to rotational damping, shortly after the completion of its roll-up, in amounts proportional to the vorticity in the core. The critical parameters controlling the rotational damping in a nonstratified medium appear to be  $Rec = \Gamma/\nu$  and  $Ro = (U_\infty - U_{cl})/V_m$ . It may be postulated that there are critical values of  $Rec$  and Rossby number above which the rotational damping occurs. Should this be true, the said damping should decrease with time.

The rotational damping is accompanied by mass, momentum, and vorticity exchange between the inner and outer regions of the core, as evidenced by several experimental and numerical studies.



Fig. 18 Evolution of helical structures around the core of a vortex.

Sarpkaya<sup>22–24</sup> observed that sheets of helical vorticity sprout out of the edges of the vortex core, transform into isolated turbulent patches or packets, and subsequently get thrown out from the edges of the core in the direction of rotation. Figure 18 shows a sample photograph of the vortex core and its edges, generated by a NACA 0012 foil (at 6-deg angle of attack and rounded tips) in a high-speed water tunnel. The flow visualization was made through the use of fluorescent dyes with high Schmidt numbers (dye was introduced only at the axis of the vortex) and 5-mm round Polyamid<sup>®</sup> particles of specific gravity of 1.02 (introduced outside the core). A thin monochromatic laser light sheet (about 250 mm thick and 250 mm wide with a wavelength of 532 nm) was provided by a Nd-YAG laser with a pulse duration of 6 ns. The Reynolds number of the vortex was  $Re_c = 9 \times 10^4$  and  $Ro = (U_\infty - U_c)/V_m = 0.76$ . The TKE level of the ambient flow was about 2.5%. Figure 18 shows that sheets of helical vorticity spiral off from the edges of the core. The fact that these structures are helical in nature is better appreciated by recording the vortex with a high-speed imager and then viewing it at a lower speed, as we have done. The structures may be made more or less intense by increasing or decreasing the turbulence level of the ambient flow through the use of suitable grids. The particles introduced outside the core (with no dye in the core) migrated intermittently into the core, even though they had a specific gravity of 1.02, showing that indeed there is mass exchange between the core and its surroundings. This is an inertial mechanism and does not need diffusion for its existence.

The experimental evidence is that the core of a vortex, surrounded by a turbulent environment, is not a benign, smooth, axisymmetric, solid body in rotation. The core is, as it must be, replenished with fresh (turbulent) fluid from the outer region. In other words, a turbulent exchange of momentum must take place between the outer region and the core. It is this exchange of mass, momentum, and vorticity between the outward flux of intense core vorticity (in intermittently shed patches) and the inward flux of replenishing turbulent fluid, bearing lesser vorticity, that leads to the decay of the core vorticity through an inertial mechanism. In this process, the role of molecular diffusion is thought to be negligible. However, the role of the axial velocity is thought to be of special importance.<sup>18,19</sup> It surrounds the core (with maximum stresses near  $2Rcv/3$ ) with an intense shear layer that serves as a source of turbulence, in addition to that initially wrapped around the core and to the ambient turbulence interacting with the vortex. Thus, the means to increase the axial velocity may contribute to higher turbulence and faster circulation decay.

Bandyopadhyay et al.<sup>19</sup> have made similar observations on a trailing vortex, generated by a pair of oppositely loaded airfoils in the longitudinal plane of a cylinder in a low-speed boundary-layer channel. The freestream turbulence was produced by screens and grids located downstream of the contraction and at a sufficient distance upstream of the model. The measurements and flow visualization were carried out at an axial distance of  $x = 40c$ . Bandyopadhyay et al. observed that “there is an intermittent exchange of momentum between the outer and the core regions. The core receives a patch of turbulent fluid and the rotational motion partially relaminarizes it.” However, the range of their Reynolds numbers was lower than that needed to effect a change in the turbulence structure. They also noted that the shear-stress-rich low-momentum core fluid (small three-dimensional packets of vorticity) is ejected intermittently outward in the direction of vortex rotation.

Among others, Ragab and Sreedhar<sup>20</sup> used large-eddy simulation to show that a single  $q$ -vortex with axial velocity deficit is unstable, at least temporarily, to random and controlled disturbances. The

instability gives rise to large-scale helical structures sprouting out of the vortex core and causes radial exchange of angular momentum. However, during the period of growth of disturbances, the mean tangential velocity shows no significant decay, whereas the axial velocity deficit weakens appreciably. This results in a stabilizing mean flow that quenches the large-scale motions, and the vortex returns to a laminar configuration.

Risso et al.<sup>21</sup> carried out a three-dimensional direct numerical simulation of the interaction between a pair of Lamb–Oseen vortices and a homogeneous turbulence field for  $t^* < 160$  and  $Re_v = 6 \times 10^2$ , which is about four orders of magnitude smaller than that of a real vortex (see Fig. 10). Risso et al. concluded that the role of the large and small turbulent scales can be separated into two independent mechanisms. 1) The turbulent transport of small scales manifests itself as an increase of the effective diffusion. 2) The vortex stretching process transfers vorticity from the vortex to the ambient turbulence. “This causes the decrease of the global intensity of the vortex and, thus, the circulation decays.” Presumably, the decay implies the draining of vorticity out of the Kelvin oval and/or the annihilation of vorticity in the overlapping regions of vortices. Risso et al. noted that the vortex stretching is an inertial mechanism and acts on all of the turbulent scales but the major part of the entropy is given to the large scales, which are independent of viscosity and can be significantly stretched before reaching the dissipative scales. They argued that “the prediction of the circulation is sufficient in practical problems, but it is necessary to relate it to the vortex stretching mechanism and not to the properties of diffusion of turbulence.” Their predictions, confined to very small times and Reynolds numbers ( $Re_v = 6 \times 10^2$ ), are not comparable with the field data presented herein. Nevertheless, the stretching of the fluid elements outside the core, especially in the overlapping regions of the vortices, is important and leads to the annihilation of oppositely signed vorticity.

The additional decay of the circulation at any time and radial distance requires that the Kelvin oval be a loosely woven basket rather than a rigid container. It is only then that the vorticity can be entrained and detained. The entire decay process, with or without stretching, is subjected to turbulent diffusion particularly at smaller scales. In other words, the vorticity transferred from the vortex to the ambient turbulence by the stretching process eventually reduces to smaller scales by turbulent diffusion. Thus, stretching is not a new model but an intermediate step to the ultimate diffusion of vorticity and decay of vortex. As the vorticity in the outer regions of the core diminishes and the external velocity profile becomes more potential like, the velocity near the edge of the core becomes higher than those extrapolated from the exterior potential vortex field. This is the cause of the helical instabilities that lead to mass, momentum, and vorticity exchange between the inner and outer regions of the core. Buoyancy-generated counter sign vorticity, wind shear, and ground effects are expected to further enhance the demise mechanisms.

## Conclusions

The analysis of representative field data in light of the knowledge gained from the existing laboratory and numerical experiments suggested the following conclusions:

1) The effect of the molecular diffusion on the downwash and the demise of trailing vortices is inconsequential and inconsistent with the high-Reynolds-number field data.

2) The vortex core is not a benign solid body in rotation. There is an intermittent exchange of mass, momentum, and vorticity across the core boundary. This process may be enhanced by mutual straining, rotational damping and restructuring of turbulence, helical instability, atmospheric turbulence surrounding the vortex, axial velocity, interaction of oppositely signed vorticity in the overlapping regions of the vortex pair, draining of vorticity from the Kelvin oval, stratification effects, wind shear, and ground effects.

3) Large flow structures outside the core are stretched by velocity gradients induced by the vortex pair. The vorticity transferred from the vortex to the ambient turbulence by the stretching process eventually reduces to smaller scales by turbulent diffusion.

4) Some but not all of the governing parameters may be made to attain critically high enough values in small-scale physical and numerical experiments. Field experiments are absolutely indispensable



to create the conditions that sustain a critical damping mechanism. This is in spite of their shortcomings and the vagaries of the meteorological conditions. The acquisition of detailed turbulent kinetic energy, dissipation, and axial velocity data must be given high priority for they will shed additional light on the physics of the decay mechanisms of trailing vortices and, equally important, on the evolution of reliable large-eddy simulations.

5) Any attempt to enhance the decay of vortices must strive to intensify the turbulence near the core, the helical instabilities at the edge of the vortex, and the axial velocity.

### Acknowledgments

The support of this investigation by the NASA Langley Research Center under Contract L-66791D, with R. Brad Perry and F. H. Proctor as Technical Monitors, is greatly appreciated. Special thanks are extended to J. S. Brown and M. Murat for their assistance with the calculations.

### References

- <sup>1</sup>Hallock, J. N., "Aircraft Wake Vortices: An Assessment of the Current Situation," U.S. Dept. of Transportation, DOT-FAA-RD-90-20, DOT-VNTSC-FAA-90-6, Federal Aviation Agency, Washington, DC, May 1991.
- <sup>2</sup>Greene, G. C., Dunham, R. E., Jr., Burnham, D. C., Hallock, J. N., and Rossow, V. J., "Wake Vortex Research: Lessons Learned," *Proceedings of the Aircraft Wake Vortices Conference*, DOT/FAA/SD-92/1.1, U.S. Dept. of Transportation Volpe National Transportation Systems Center, Cambridge, MA, 1992, pp. 2-1-2-13.
- <sup>3</sup>"FAA International Wake Vortex Symposium," DOT/FAA/SD-92-1, Federal Aviation Agency, Washington, DC, July 1991.
- <sup>4</sup>MacCready, P. B., Jr., "An Assessment of Dominant Mechanisms in Vortex-Wake Decay," *Aircraft Wake Turbulence and Its Detection*, 1st ed., Plenum, New York, 1971, pp. 289-304.
- <sup>5</sup>"The Characterization and Modification of Wakes from Lifting Vehicles in Fluids," CP-584, AGARD, May 1996.
- <sup>6</sup>Sarpkaya, T., "Trailing Vortices in Homogeneous and Density Stratified Media," *Journal of Fluid Mechanics*, Vol. 136, Nov. 1983, pp. 85-109.
- <sup>7</sup>Tombach, I., "Observations of Atmospheric Effects of Vortex Wake Behavior," *Journal of Aircraft*, Vol. 10, No. 11, 1973, pp. 641-647.
- <sup>8</sup>Sarpkaya, T., and Daly, J. J., "Effect of Ambient Turbulence on Trailing Vortices," *Journal of Aircraft*, Vol. 26, No. 6, 1987, pp. 399-404.
- <sup>9</sup>Liu, H.-T., "Effects of Ambient Turbulence on the Decay of a Trailing Vortex Wake," *Journal of Aircraft*, Vol. 29, No. 2, 1992, pp. 255-263.
- <sup>10</sup>Crow, S. C., and Bate, E. R., "Lifespan of Trailing Vortices in a Turbulent Atmosphere," *Journal of Aircraft*, Vol. 13, No. 7, 1976, pp. 476-482.
- <sup>11</sup>Crow, S. C., "Stability Theory for a Pair of Trailing Vortices," *AIAA Journal*, Vol. 8, No. 12, 1970, pp. 2172-2179.
- <sup>12</sup>Han, J., Lin, Y.-L., Schowalter, D. G., Arya, S. P., and Proctor, F. H., "Large-Eddy Simulation of Aircraft Wake Vortices: Atmospheric Turbulence Effects," *12th Symposium on Boundary Layers and Turbulence* (Univ. of British Columbia, Vancouver, BC, Canada), American Meteorological Society, Boston, MA, 1997, pp. 237, 238.
- <sup>13</sup>Zak, J. A., and Rogers, W. G., Jr., "Documentation of Atmospheric Conditions During Observed Rising Aircraft Wakes," NASA CR-4767, April 1997.
- <sup>14</sup>Campbell, S. D., Dasey, T. J., Freehart, R. E., Heinrichs, R. M., Matthews, M. P., Perras, G. H., and Rowe, G. S., "Wake Vortex Field Measurement Program at Memphis, TN Data Guide," Lincoln Lab., Massachusetts Inst. of Technology, Project Rept. NASA/L-2, Lexington, MA, Jan. 1997 (available to the public through the NTI Service, Springfield, VA 22161).
- <sup>15</sup>Batchelor, G. K., "Axial Flow in Trailing Line Vortices," *Journal of Fluid Mechanics*, Vol. 20, Dec. 1964, pp. 645-658.
- <sup>16</sup>Moore, D. W., and Saffman, P. G., "Axial Flow in Laminar Trailing Vortices," *Proceedings of the Royal Society of London*, Vol. 33A, June 1973, pp. 491-508.
- <sup>17</sup>Thompson, D. H., "Experimental Study of Axial Flow in Wing Tip Vortices," *Journal of Aircraft*, Vol. 12, No. 11, 1975, pp. 910, 911.
- <sup>18</sup>Uberoi, M. S., Shivamoggi, B. K., and Chen, S., "Axial Flow in Trailing Line Vortices," Purdue Univ., Project Squid TR UC-2-PU, Lafayette, IN, July 1978.
- <sup>19</sup>Bandyopadhyay, P. R., Stead, D. J., and Ash, R. L., "Organized Nature of a Turbulent Trailing Vortex," *AIAA Journal*, Vol. 29, No. 10, 1991, pp. 1627-1633.
- <sup>20</sup>Ragab, S. A., and Sreedhar, M. K., "Numerical Simulation of Vortices with Axial Velocity Deficits," *Physics of Fluids A*, Vol. 7, March 1995, pp. 549-558.
- <sup>21</sup>Risso, F. R., Corjon, A., and Stoessel, A., "Direct Numerical Simulations of Wake Vortices in Intense Homogeneous Turbulence," *AIAA Journal*, Vol. 35, No. 6, 1997, pp. 1030-1040.
- <sup>22</sup>Sarpkaya, T., "Three-Dimensional Interactions of Vortices with a Free Surface," AIAA Paper 92-0059, Jan. 1992.
- <sup>23</sup>Sarpkaya, T., "Interaction of a Turbulent Vortex with a Free Surface," *Proceedings of the Nineteenth Symposium on Naval Hydrodynamics*, Vol. 1, National Academy Press, Washington, DC, 1992, pp. 163-174.
- <sup>24</sup>Sarpkaya, T., "Vorticity, Free Surface, and Surfactants," *Annual Review of Fluids Mechanics*, Vol. 28, 1996, pp. 83-128.
- <sup>25</sup>Heinrichs, R. M., and Dasey, T. J., "Analysis of Circulation Data from a Wake Vortex Lidar," AIAA Paper 97-0059, Jan. 1997.
- <sup>26</sup>Hinton, D. A., "Aircraft Vortex Spacing System (AVOSS) Conceptual Design," NASA TM-110184, Aug. 1995.
- <sup>27</sup>Perry, R. B., Hinton, D. A., and Stuever, R. A., "NASA Wake Vortex Research for Aircraft Spacing," AIAA Paper 97-0057, Jan. 1997.
- <sup>28</sup>Proctor, F. H., "Numerical Simulation of Wake Vortices Measured During the Idaho Falls and Memphis Field Programs," AIAA Paper 96-2496, June 1996.
- <sup>29</sup>Proctor, F. H., Hinton, D. A., Han, J., Schowalter, D. G., and Lin, Y.-L., "Two-Dimensional Wake Vortex Simulations in the Atmosphere: Preliminary Sensitivity Studies," AIAA Paper 97-0056, Jan. 1997.
- <sup>30</sup>Vicroy, D., Brandon, J., Greene, G., Rivers, R., Shah, G., Stewart, E., and Stuever, R., "Characterizing the Hazard of a Wake Vortex Encounter," AIAA Paper 97-0055, Jan. 1997.
- <sup>31</sup>Longuet-Higgins, M. S., and Cokelet, E. L., "The Deformation of Steep Surface Waves on Water. I. A Numerical Method of Computation," *Proceedings of the Royal Society of London, Series A*, Vol. 350, July 1976, pp. 1-26.
- <sup>32</sup>Hallock, J. N., and Burnham, D. C., "Decay Characteristics of Wake Vortices from Jet Transport Aircraft," AIAA Paper 97-0060, Jan. 1997.
- <sup>33</sup>Owen, P. R., "The Decay of a Turbulent Trailing Vortex," *Aeronautical Quarterly*, Vol. 21, Feb. 1970, pp. 69-78.
- <sup>34</sup>Lezius, D. K., "Water Tank Study of the Decay of Trailing Vortices," *AIAA Journal*, Vol. 12, No. 8, 1974, pp. 1065-1071.
- <sup>35</sup>Greene, G. C., "An Approximate Model of Vortex Decay in the Atmosphere," *Journal of Aircraft*, Vol. 23, No. 7, 1986, pp. 566-573.
- <sup>36</sup>Traugott, S. C., "Influence of Solid-Body Rotation on Screen-Produced Turbulence," NACA TN-4135, April 1958.
- <sup>37</sup>Briggs, D. C., "Heat Transfer in Rotating Turbulent Pipe Flow," Dept. of Mechanical Engineering, Stanford Univ., TR 45, Stanford, CA, May 1959.
- <sup>38</sup>Hopfinger, E. J., Browand, F. K., and Gage, Y., "Turbulence and Waves in a Rotating Tank," *Journal of Fluid Mechanics*, Vol. 125, Dec. 1982, pp. 505-534.
- <sup>39</sup>Polifke, W., and Shtilman, L., "The Dynamics of Helical Decaying Turbulence," *Physics of Fluids A*, Vol. 1, No. 12, 1989, pp. 2025-2033.

A. Plotkin  
Associate Editor